SANDIA REPORT
SAND2020-9593
Printed September 2020

Big-Data-Driven Geo-Spatiotemporal Correlation Analysis between Precursor Pollen and Influenza and its Implication to Novel Coronavirus Outbreak

Michael G. Wallace
Yifeng Wang

Prepared by
Sandia National Laboratories
Albuquerque, New Mexico
87185 and Livermore,
California 94550

Issued by Sandia National Laboratories, operated for the United States Department of Energy by National Technology & Engineering Solutions of Sandia, LLC.

Printed in the United States of America. This report has been reproduced directly from the best available copy.

Available to DOE and DOE contractors from
U.S. Department of Energy
Office of Scientific and Technical Information
P.O. Box 62
Oak Ridge, TN 37831

Telephone: (865) 576-8401
Facsimile: (865) 576-5728
E-Mail: reports@osti.gov
Online ordering: http://www.osti.gov/scitech

Available to the public from
U.S. Department of Commerce
National Technical Information Service
5301 Shawnee Rd
Alexandria, VA 22312

Telephone: (800) 553-6847
Facsimile: (703) 605-6900
E-Mail: orders@ntis.gov
Online order: https://classic.ntis.gov/help/order-methods/

ABSTRACT

Although studies of many respiratory viruses and pollens are often framed by both seasonal and health related perspectives, pollen has yet to be extensively examined as an important covariate to seasonal respiratory viruses (SRVs) in any context, including a causal one. This study contributes to those goals through an investigation of SRVs and pollen counts at selected regions across the Western Hemisphere. Two complementary decadal-scaled geospatial profiles were developed. One laterally spanned the US and was anchored by detailed pollen information for Albuquerque, New Mexico. The other straddled the equator to include Fortaleza, Brazil. We found that the geospatial and climatological patterns of pollen advancement and decline across the US every year presented a statistically significant correlation to the subsequent emergence and decline of SRVs. Other significant covariates included winds, temperatures, and atmospheric moisture. Our study indicates that areas of the US with lower geostrophic wind baselines are typically areas of persistently higher and earlier influenza like illness (ILI) cases. In addition to that continental-scaled contrast, many sites indicated seasonal highs of geostrophic winds and ILI which were closely aligned. These observations suggest extensive scale-dependent connectivity of viruses to geostrophic circulation. Pollen emergence and its own scale-dependent circulation may contribute to the geospatial and seasonal patterns of ILI. We explore some uncertainties associated with this investigation, and consider the possibility that in a temperate climate, following a Spring pollen emergence, a resulting increase in pollen triggered human Immunoglobulin E (IgE) antibodies may suppress ILIs for several months.

ACKNOWLEDGEMENTS

We wish to acknowledge and express our appreciation to Jennifer Frederick and Philippe F. Weck for the technical review of this study and to Gil Herrera for his leadership in helping us to navigate from the beginning through to the conclusion of this investigation. We also appreciate the critical support and contributions of many other SNL management and staff including, Erik Webb, Chris Camphouse, Tracy Woolever, Carol Adkins, Emily Stein, Darielle Dexheimer, Adah Wang, and Bryan Carson. We are additionally indebted to Dan Gates, senior environmental health scientist of the City of Albuquerque Environmental Health Department, and Emma Stanislawski, MPH, CPH, Respiratory Infections Surveillance Epidemiologist, Epidemiology Response Division of New Mexico Department of Health. Their carefully documented data archives of pollen and Influenza Like Illnesses (ILI) for the Albuquerque Metropolitan area were crucial to the advancement of this work. This acknowledgement does not constitute an endorsement from any of those parties. This work was supported by Sandia's Laboratory-Directed Research and Development (LDRD) Program.

CONTENTS

Table of Figures

This page left blank

ACRONYMS AND DEFINITIONS

Abbreviation	Definition
CDC	US Centers for Disease Control and Prevention
CLI	Covid-19 Like Illness
EP	Evaporation minus precipitation
IgE, IgG, IgM	Immunoglobulin E, G and M antibodies
ILI	Influenza Like Illness
LEDIV	Divergence of Latent Energy
SEIR	Susceptible – Exposed – Infectious – Recovered. Agent-based virus transmission models
SRV	Seasonal Respiratory Virus
UCAR ERAI	University of California at Riverside integration of data from ERA-Interim project Europe.
WHO	World Health Organization

1. INTRODUCTION

Regardless of the shortcomings of current vaccination practices, seasonal patterns clearly indicate that some common factor(s) may diminish the outbreak or spreading of respiratory-related viruses. This has been evident, whether a vaccine was utilized or not. The seasonal diminishment is believed to apply to all relevant influenza, adeno, and coronaviruses (though its effect on the current Covid-19 outbreak remains to be seen). These seasons are typically the summer in temperate latitudes and the dry season(s) in the tropics. A further clarification of the controlling climatic and environmental factors would at the very least improve forecasting of respiratory viral outbreaks and declines and therefore help to inform future flu mitigation efforts.

Seasons are a manifestation of atmospheric conditions, and earlier research by Hammond et al, (1989) and, to a lesser extent, by Lofgren et al, (2007) have attempted to relate atmospheric circulation patterns to seasonal respiratory viruses (SRVs). Hammond et al. (1989) hypothesized viruses as drifting “accumulation mode” particles which could be widely distributed through the atmosphere and could circulate in part according to their sizes. Conceptual models along these lines also sought to explain various types of sudden and extensive viral outbreaks covering vast regions. These flareups seemed difficult to explain through conventional person to person (agent-based) transmission evaluations. Whon et al. (2012) was the first to report the seasonality of airborne viruses and their genetic diversity. Recent investigations by Reche et al. (2018) further demonstrated the exceptional variety and intensity of viral flux through the planetary boundary layer at two sites within Spain’s Sierra Nevada Mountains.

Conventionally, both transmission and survivability topics of viruses were merged in past studies, and the assumed primacy of agent-based transmission was rarely tested. For example, recent work by Tamerius et al. (2013), Shaman et al. (2009; 2017) and Su et al. (2020) assert that humid air slows transmission of an influenza virus in temperate zones. Some work also indicates that dry and cold air can stimulate virus transmission or at least not interfere with it (Shaman et al. (2009). Yet rainy seasons in tropical regimes are also humid seasons, and those can be the times in those latitudes when influenza is most prevalent.

As suggested in this report, pollen counts in atmosphere could be a promising additional environmental factor for consideration with regard to the seasonality of viral outbreaks. It is important to note that pollen is an antigen. There is abundant literature that have shown, usually separately, the innate immune responses of human tissues to pollen and the active immune responses to respiratory viruses (Hosoki et al., 2015, Lee et al., 2016, Pawankar et al., 2011, Smith-Norowitz et al., 2012). Some evidence is found to date for cross reactivity between Immunoglobulin E (IgE) antibodies associated with allergens, and the viral Immunoglobulin G and M (IgG and IgM) antibodies, thus pointing out a possibility that human body response to allergens may provide temporary immunity to a respiratory virus. In the work presented below, we will test a simple hypothesis that pollen counts, coupled with seasonal atmospheric transport of virus, can provide a reasonable explanation for the seasonal spread and decline of all common respiratory viruses, including the novel coronavirus SARS-CoV-2. If confirmed, this hypothesis may lead to more accurate forecasts of viral patterns, as well as a new perspective for inhibiting the spread of influenza, or any coronavirus, for example, using pollen to induce an immunity-strengthening response in humans.

2. METHODS

We focused on publicly available data to explore an intersection between climate, pollens and SRVs. Standard statistical methods were used to evaluate the statistical significance of pollen and SRV correlations. In these exercises, the covariation of seasonal pollens with SRVs from year to year and across selected climatological zones were developed. Figure 1 features our primary subject of two pollen time series (blue and green dots) and one SRV series (red dots), for Albuquerque, New Mexico in the US, based upon resources provided directly by the City of Albuquerque (2020) and the New Mexico Department of Health (2020). The pollen series represent 20 years of sampling on a routine and often daily basis. The following species of pollen were sampled at both the east Albuquerque site (blue dots) and the west Albuquerque site (green dots): Ash, Chenopodiaceae, Grass, Mulberry, Pine, Rumex, Aster, Cottonwood, Juniper, Oak, Ragweed, Willow, Birch, Elm, Maple, Ephedra (Mormon Tea) and Sagebrush. The green and blue dots signify totals for all pollen species in every sampling day over that period. A log scale is used to capture the wide spread of numbers for both series.

Figure 1 also details a time series of New Mexico influenza like illness (ILI) counts specific to hospitalization and related reports over the same 20-year time frame. These numbers were developed from information routinely consolidated into weekly reports by the New Mexico Department of Health and shared with the US Centers for Disease Control and Prevention (CDC) in the development of their "FLUView" ILI dashboard [CDC 2020a]. ILI reports primarily stem from records of serious respiratory illness accompanied by diagnostic measures up to actual RNA testing for specific virus strains. Numbers that feed into ILI and the new CLI (Covid-19 related illnesses, via their COVIDView dashboard [CDC 2020b]), are assumed in this investigation to be reliable signatures of the amplitude and spread of SRVs. Accordingly, these records might also serve as a potential proxy for the actual geospatial transport and persistence of SRVs in the atmosphere. If true that would add significant value because virus monitoring in the atmosphere is not yet widespread or practical.

As we subsequently show, seasonal atmospheric transport of viruses could be an important process that needs to be considered in understanding seasonality of influenza outbreak and spreading. Vertical and lateral circulations of winds and the viruses they carry are no doubt challenging to map. Fortunately, as demonstrated for example in Wallace (2019), the dynamics of climate systems can be geostrophically simplified without sacrificing critical information including winds, temperatures, pressures (and geopotential heights), and the changes in latent heat associated with any air parcel. In the widely used geostrophic approximation, each parcel of air starts as a rectangular footprint above the land or ocean surface and extends to the top of the atmosphere (TOA) roughly 100 km in altitude. In spite of the larger synoptic scale that their use is limited to, geostrophic approximations closely resemble observations of many surface weather features regardless of boundary layers, shears, vortexes or baroclinicity. Geostrophic datasets are accordingly an important component exercised in this study, not only because their signatures may capture higher altitude virus transport conditions, but also because the UCAR ERAI dataset (University of California at Riverside 2015) allows for the direct interrogation of any part of the planet's atmospheric footprint for any month over a recent 36-year period. Surface weather records in comparison are far more difficult to assemble outside of major metropolitan regions. Because of the characteristics of reproducibility and continuity, in this study geostrophic assets where convenient are also compared to equivalent surface records.

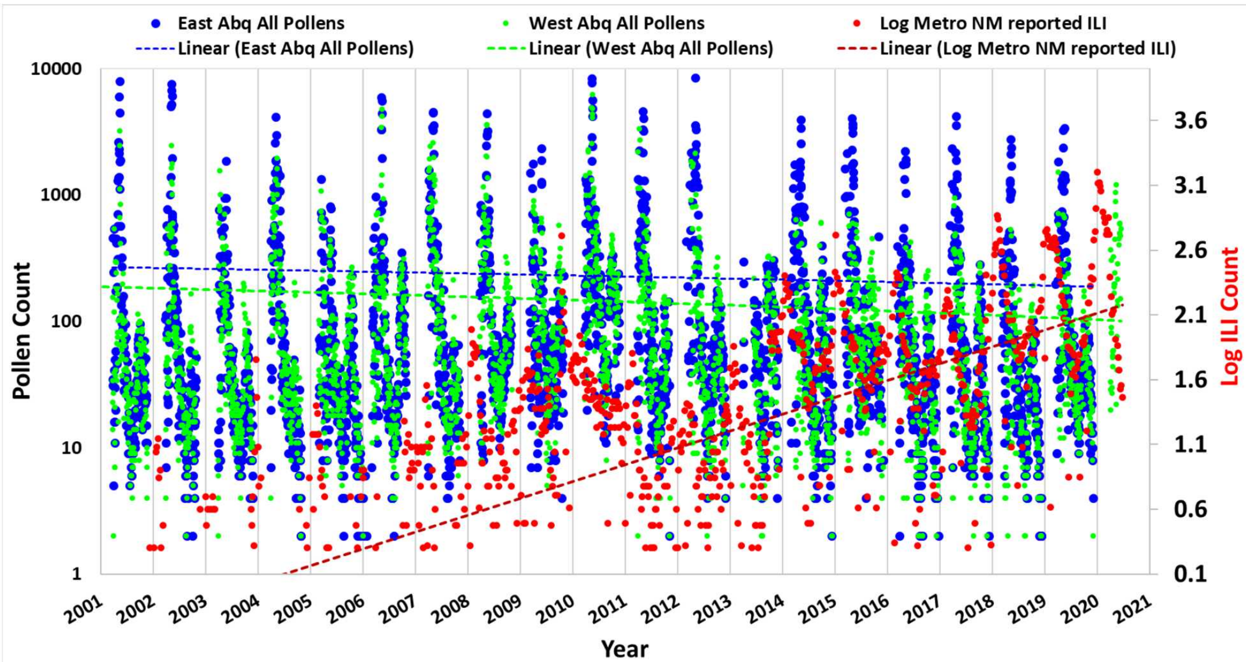

Figure 1. Comparison of reported ILIs to records of two pollen monitoring stations for Albuquerque, NM, US. Source: City of Albuquerque, Environmental Health Department. Air Quality Program. https://www.cabq.gov/airquality and New Mexico Department of Health. Epidemiology and Response Division. www.nmhealth.org

3. RESULTS

Seasonal correlation of ILI with pollen counts and other climatological variables. Many patterns are graphically apparent in the two bioaerosols (viruses and pollens) plotted in Figure 1. It is obvious that western Albuquerque which is more exposed to westerly winds from adjacent arid lands, has lower pollen levels than the more developed urban eastern pollen station. Also, by virtue of the general arid domain surrounding Albuquerque, both series show lower ranges of pollen than many other sites throughout the wetter central and eastern US. The blue and green trend lines also indicate that both pollen series have slightly (on a logarithmic scale) dropped over time in a city that has grown moderately over that same period. The red trendline for the Albuquerque ILI record provides an interesting comparison to the pollen time series. Peaks of ILI occur in the winters, and these peaks have been growing in amplitude over the past several years. Accordingly, as pollen trends have stayed relatively subdued, the incidence of ILI has risen. It is also apparent from this figure that flu seasons peak between pollen seasons, and vice versa, indicating a clear inverse correlation between the pollen counts and ILI.

Concern over the ongoing trend of rising ILI in spite of rising vaccination rate has received some attention in the health sciences literature (Fukushima and Hirota, 2017, Spruijt et al., 2016). This trend has been consistent across the US for decades. There is no easy explanation for this trend. If some long-term environmental shifts such as the decline of annual average pollen counts (Figure 1) were a factor, this ILI trend could not be identified through the current SEIR (Susceptible Exposed Infectious Recovered agent-based virus transmission models) rooted paradigm for SRV epidemiology.

Figure 2 details the correlations of ILI with pollen and other climatological variables for Albuquerque, New Mexico, USA and Fortaleza, Brazil. These charts track the average monthly condition of selected variables over the multiple year data collection time period. The Fortaleza location is also indicated in Figure 3b by the open black circle at the northeast location of the South American zone. Fortaleza is selected because of past relevant studies as well as its tropical southern hemisphere position for comparison to the US patterns. Published information (Tamerius, 2013) along with routine weather reporting indicates a high correlation between SRVs and atmospheric moisture (rain) for that tropical location. That high correlation, along with each other significant weather and ILI correlation for the two sites are summarized in Figure 2c.

The Brazilian studies also describe that for each flu season ILIs emerge near Fortaleza and then migrate southward along the Brazilian coast every winter. Correlations of ILI to tropical airborne pollens may remain challenging because those winds are much lower in general intensity than temperate surface winds. Tropical pollen long term monitoring methodologies are typically less than successful for this very reason (Behling and Negrelle, 2006, and Caraballa et al., 2016). Accordingly, a pollen "rain" is often described, to represent that pollens do not appear to be windblown very far from any plant in tropical locations. In spite of those obstacles, it is clear that pollen producing plants are abundant in tropical regions. Greco and Lima (1941) reports that pollination peaks in May in the Rio Di Janeiro area. That pollen peak is represented by a transparent green column in Figure 4b.

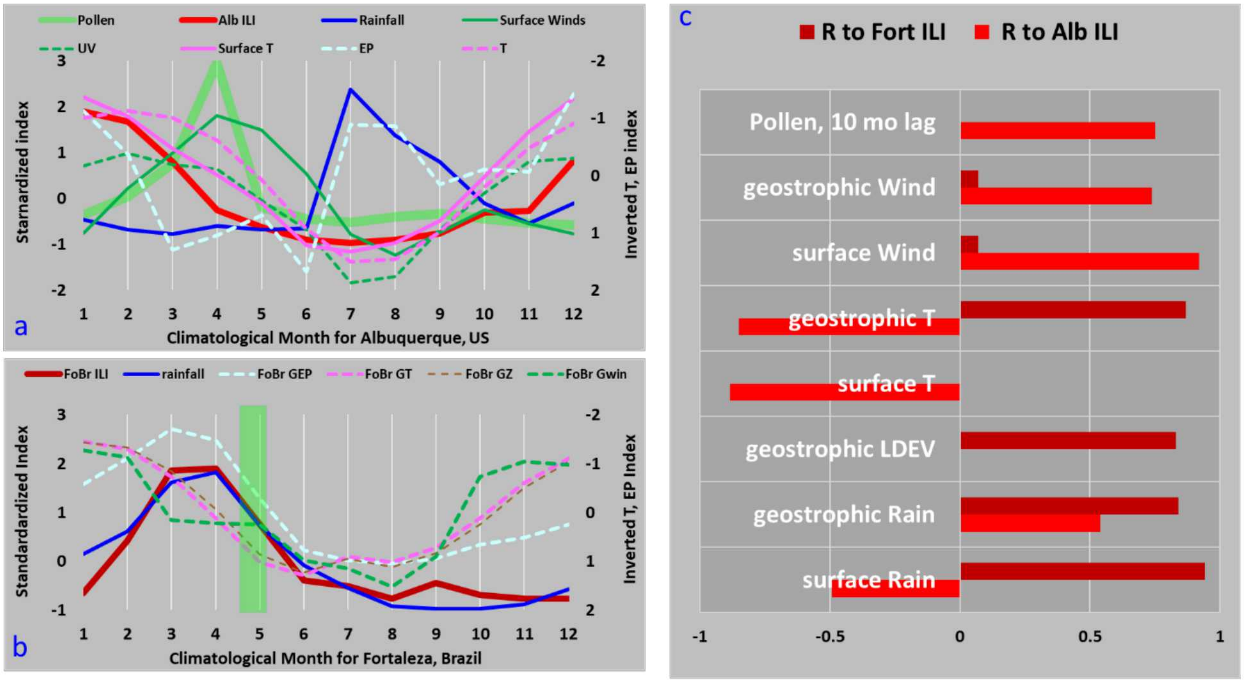

Figure 2. Seasonal variations of standardized climatological variables and their correlations with ILI for two sites in the Western Hemisphere. a. Albuquerque, US. b. Fortaleza, Brazil. c. Correlation coefficients. The data in a and b are averaged over the multiple year data collection time period.

As shown in Figures 2a and 2b, many aspects of the Albuquerque and the Fortaleza climatology curves appear similar when factoring a two-to-three-month shift in general, as well as the North American Monsoon impact on rainfall in Albuquerque. Otherwise both curves indicate a similar alignment between the geostrophic and surface wind sets (dark green solid for the surface and dotted green line for geostrophic). The data from both sites clearly indicate that as pollen emerges in the early part of each climatological year, ILI peaks begin to decline. Moreover, several months after pollen peaks decline, ILI counts begin again to rise. That is, pollen concentrations trend inversely with viral outbreak episodes in both climate regimes. Their concentration declines in temperate climates during the winter because pollens are not produced then. In tropical climates, even as vegetation continues to grow, the rainy seasons can be persistent and nearly continuous, thereby removing pollens quickly from the atmosphere. Figure 4c summarizes the correlations of various climatological variables to ILI that are significant for both the Albuquerque (bright red) and the Brazlian (dark red) ILI patterns. Although winds are much less intense (and correlated) in tropical locations, rainfall is much more intense (and more correlated). As discussed below, the susceptibility of any lofted particle in the atmosphere depends on the particle size. In comparison to viruses, pollens are relatively easily removed from the atmosphere by rain. It is true that in temperate regions, winds can make a difference. But in the tropics, due to the lower winds and higher rains, pollens likely cannot circulate through those regions as robustly as they migrate through temperate zones.

We compared geostrophic information with the UCAR ERAI data for both Brazil and Albuquerque, the light blue dotted lines which represent Evaporation minus Precipitation (EP) for the full atmosphere, closely follow the dark blue solid lines (rainfall at surface) (Figures 2a and 2b). This comparison helps add confidence to the use of geostrophic information in comparing weather to SRVs. The divergence of latent energy (LEDIV) (Wm^{-2}) was also plotted and, as expected, it also aligned to the other moisture parameters. In addition to the wind and moisture variables, geostrophic temperatures (dotted pink lines) display high similarities to surface temperatures (solid pink lines) at both locations, although their relations to ILI vary across the equator for these sites.

Figure 2c summarizes the correlation condition (R) via the Pearson's correlation test for each statistically significant comparison of the weather and pollen variables to the ILI index for Fortaleza (dark red) and Albuquerque (bright red). Because all variables are normalized first and because there are 12 entries per variable for each test, any R value greater than .5 is statistically significant. It is evident that SRVs and each category of weather and pollen variable are connected, but that the strength and direction of the relations can vary between temperate and tropical locations. The correlation analysis, in combination of the additional evidence to be presented below, shows that pollen appears to offer a more consistent explanation for the observed seasonal variation of viral outbreak and spreading in both climates than any other factors such as temperature and humidity. A possible causal relationship of pollen with viral outbreak may stem from the cross reactivity of antibodies induced by viruses and allergens as addressed in the Discussion section below. If this is the case, it may explain why the time lapsed between the emergence of peak pollen and the viral outbreak is approximately equal to the lifetime of allergen-induced antibodies in human bodies, which is estimated to be ~ 6 months (Figures 2a and 2b).

Geographic migration of influenza. Research which has mapped climate information to patterns of SRV illness is relatively rare. Some work based on data from Fortaleza, Brazil, has pointed out intriguing seasonal and geographic patterns of flu onset across that country (Alonso et al., 2007, Tamerius et al., 2011, Almeida et al., 2018). However, those studies generally assume an agent-based transmission paradigm, and accordingly it is sometimes argued that ILI patterns may initiate or intensify from a climate feature, but do not subsequently spread due to climate.

A unique data pattern highlighted by the three panels of Figure 3 seems to further support our hypothesis that climate and its associated pollen concentration variation could be an important contributor to the geographic emergence, transmission and decline of ILIs. Both the World Health Organization (WHO) and the CDC have occasionally noted an unexplained geospatial pattern of south to north migration of flus in temperate climates. This has also been observed within the US (Charu et al., 2017) where the authors noted "seven of eight (ILI) epidemics likely originated in the Southern US." Figure 2 summarizes our examination of this phenomenon in more detail. In this figure, geographic states east of the continental divide which best aligned to the northern and southern boundaries of the US were identified, and ILI information was developed accordingly from the CDC's FLUView resource. States featured from the south and identified by the red crosses in the geostrophic wind map of Figure 2b, were New Mexico, Texas, Louisiana, Mississippi, Alabama and Florida. States featured from the north are identified by the blue crosses in the same figure panel, which represent the centers of Montana, North Dakota, Minnesota, Vermont, New Hampshire and Maine. Figure 3a presents timelines of ILI for those two data bands, which indicate that ILI persists throughout the whole year at both southern and northern sets, but the northern set expresses a much lower ILI. This pattern seems difficult to reconcile with a traditional perception that higher ambient temperatures would tend to suppress flu virus spreading. The peaks and trends both south and north ILI time series are consistent with that for Albuquerque shown in Figure 1.

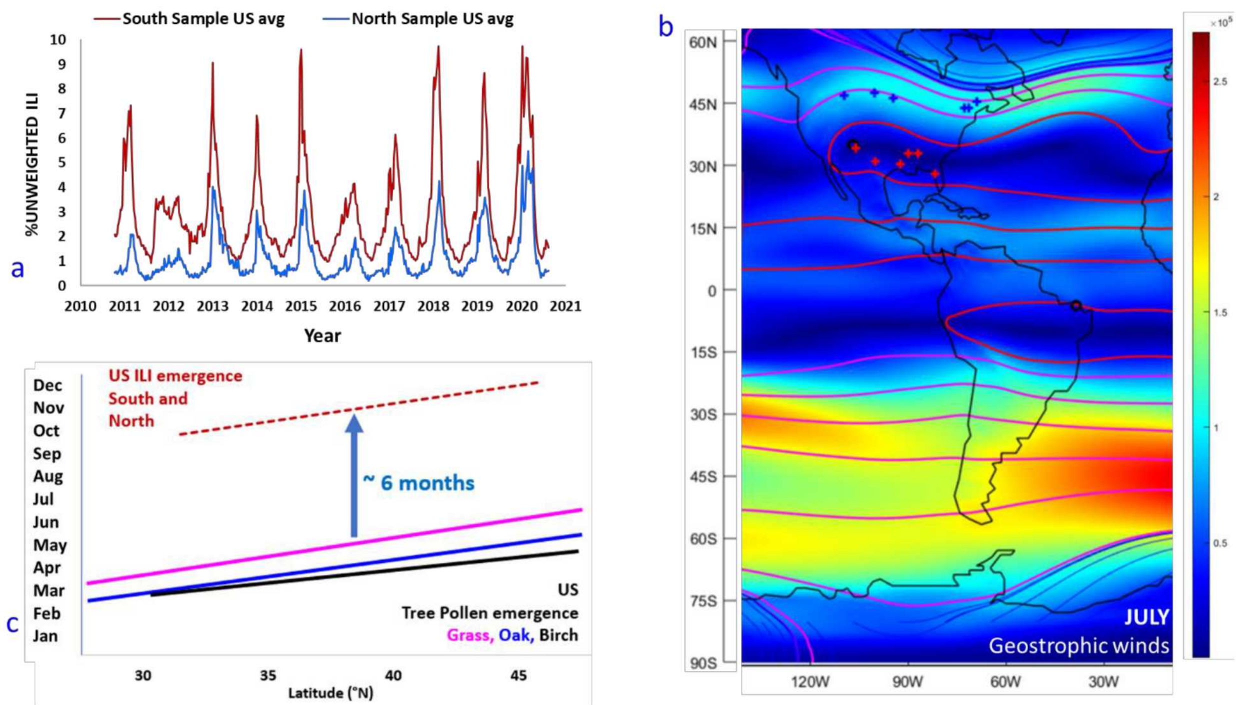

Figure 3. US ILI, Pollen, and Geostrophic Winds across the Western Hemisphere (July average). a. comparison of South Sample US ILI averages to North Samples. b. Geostrophic winds. Units: kg m^{-1} s^{-1} with streamlines. Magenta lines originate from 0 degree Long. Red lines originate from 179.5 degree Long. c. Emergence dates for ILI and Pollen across the US

In addition to identifying the State center positions across the US, Figure 3b displays the average geostrophic wind magnitude in July from the UCAR ERAI resource. As mentioned earlier, this satellite reanalysis and integration database covers 36 continuous years at a monthly resolution from 1979 through 2014. The average geostrophic wind conditions for the central months of each temperate season and the full average of all 432 months are included in the appendix of this report. As shown in Figure 3b, the July summer pattern across North America is distinctive because one of the more geostrophically stagnant zones are coincident with the southern US state band. Additional geostrophic wind maps which cover the full planet for the average months of January, April, July, and October, as well as an average annual map are included in attachment figures A1 through A5.

Figure 3c summarizes the emergence trend of the ILI pattern for the two state bands and compares this to a recently published study of the emergence trend of selected pollens (grass, oak and birch) across the same region (Zhang et al., 2015). The emergence of ILI in the figure was calculated according to the records of the southern and northern US bands by first approaching a baseline of 1% for the south and 2% for the north. The CDC resource assigns their own baseline equal to approximately 2.5%. We chose one baseline for the north and one for the south, recognizing that the ILI minima for the south are approximately twice as much as those for the north. The dates when the ILI percentage rose above those baselines were averaged for the north and south to develop the endpoints for the dotted red line in Figure 3c. In conjunction with published SRV studies, Figure 2 demonstrates some key features that discriminate pollen from all other environmental variables for causing the seasonality of influenza outbreak and spreading: (1) flu emergence consistently migrates from south to north in temperate regions; (2) the emergence trend line slopes are nearly identical, at approximately 5 days/degree latitude, for both ILI and pollens (grass and oak pollens; and (3) there exists a time lag of ~6 months between pollen exposure and a renewed flu season, which is consistent with the time lag observed at a specific geographic location (Figure 2a,b) as well as the active lifetime of known immunogens including typical SRV vaccines (Lawrence et al., 2016). This time lag could be considered as an active lifetime for antibodies induced by human allergic response to pollens. It is interesting to note a similar migration pattern can also observed in the southern hemisphere. For each flu season ILIs emerge near Fortaleza, Brazil, and then migrate southward along the Brazilian coast every winter (Tamerius et al., 2013). This is a somewhat symmetrical pattern to the US pattern outlined in Figure 3b.

One prevailing existing explanation for the seasonality of virus outbreak is a possible connection to sunlight and its enhanced vitamin D (Cannel et al., 2006). Sunlight may be particularly damaging to airborne bacteria through desiccation. The potential for photolysis to damage and/or promote mutations in both airborne viruses and microbes has also been considered (Smith, 2013). Yet, as illustrated in Figure 3, the seasonal emergence and diminishment of influenza seems to challenge this explanation, simply because warmer regions emerge into a flu season before colder zones. In addition, it is evident that in the Western US, sunshine remains abundant throughout the winter even as flu outbreaks appear to parallel those in the eastern US. And as already noted, virus prevalence seems greater in the warmer and sunnier latitudes over each temperate winter (Figure 3a).

Large-scale atmospheric transport of viruses. As shown in Figure 3a, the ILIs in both south and north bands in the US region may have different ranges, but their oscillations remain synchronized. Given the large spatial separation as well as the different circulation origins of the two geographic bands, this synchronized oscillation indicates a possible underlying mechanism for large-scale virus transport. This is consistent with the connectivity of the atmosphere in which SRVs drift. In fact as subsequently outlined, the annual (and not seasonal) fluctuations of ILI appear to be universally coherent given that the climatologically different Albuquerque and Fortaleza sites both exhibit alignments of the flu cycle to geostrophic parameters. Such consistency might be hard to explain purely through SEIR models.

Clearly viruses travel with the winds. This includes convective and advective states as well as subsidence regions that have long been mapped and continue to be studied. As shown in Figures A6 and A7, atmospheric subsidence (as indirectly suggested by the red hues) occurs over the oceans along the so-called horse latitudes. If viruses follow, that may explain observations by Reche et al. (2018) that virus loads monitored in Spain often come from the Atlantic Ocean. As noted in the southern band of US states, low geostrophic wind levels prevail over the summer, and those winds are part of a larger atmospheric gyre rooted in the Atlantic Ocean as well. The potential “pooling” of the general atmospheric virus load can be further distinguished in comparison to expected conditions of the northern state locations in Figure 3b. That northern band is aligned with the well-known North American Jet Stream, evident by the lighter color tones of the map. With stronger lateral winds comes greater lift. Whatever the transport mechanism, and depending on further observations and confirmation, a greater concentration of viral particles across the broad and diverse surfaces of the southern US every summer might then ultimately explain the greater intensity of ILI each winter in the southern band. As the direct measurements of bioaerosols expands and improves, a better understanding of virus circulation within the atmosphere is anticipated.

The geostrophic circulation and pollen-based notions introduced in this study offer a somewhat challenging but possibly complementary conceptual model to support conventional SEIR models. Among other things, the geostrophic circulation data does appear to align somewhat to the studies by Shaman et al. (2009) and perhaps most explicitly to the Hammond et al. hypothesis of virus transport. This may best be visualized through examination of the final Supplement Figures A6 (avg January LEDIV) and A7 (avg July LEDIV). The supplements on geostrophic data in Wallace (2019) also provide descriptions of geostrophic parameters covering the same time frames and spans. For LEDIV coverages, the darkest blue hues are representative in part of increased atmospheric moisture. From January to July a seasonal surge of moisture originating convectively from the West Pacific Atmospheric Warm Pool (Chen et al., 2004) reaches the temperate westerlies over China. Much as Hammond et al. outlined, air parcels (and accordingly SRVs) are transported from that footprint, across the Pacific Ocean to North America.

Virus circulation questions lead to additional relations of possible interest. For example, any geographical sources of viral loads appear to remain unspecified in common SEIR models. Origins of SRV outbreaks are sometimes characterized as zoonotic and attributed to migratory animals such as birds and bats (e.g., Chothe et al., 2017). Those flying creatures also happen to have the greatest mobilities and most extensive migrations through the atmosphere, where primary viral loads likely always reside.

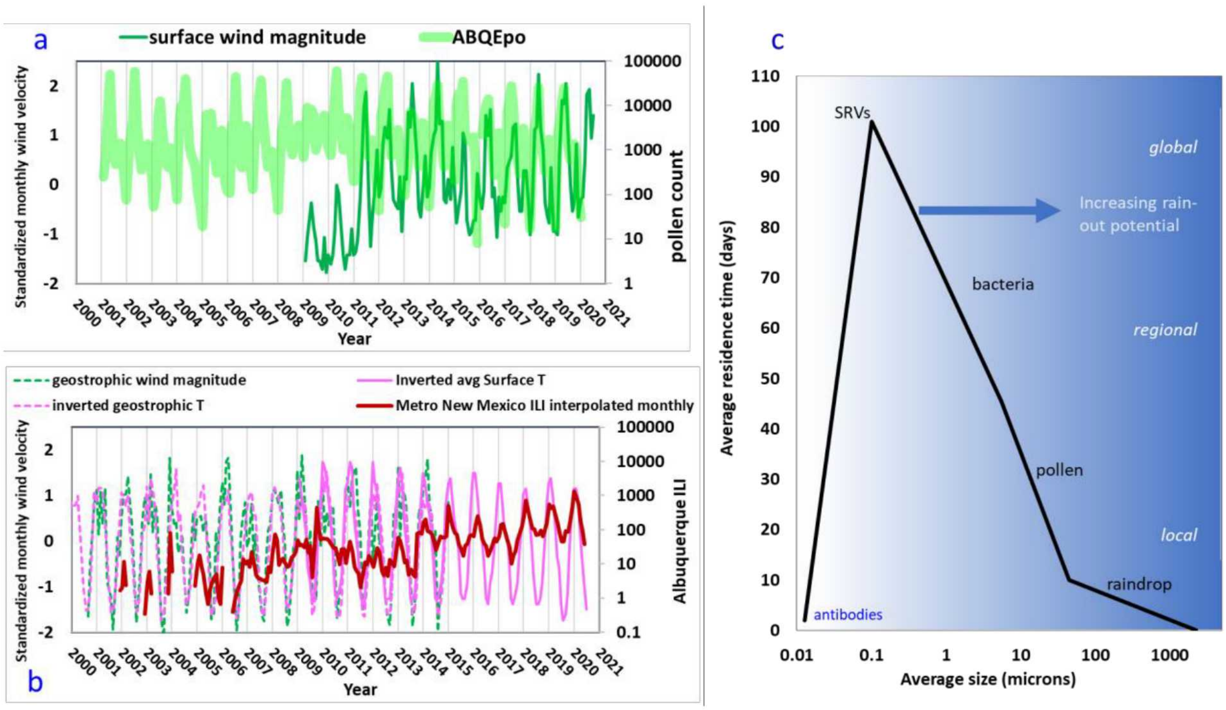

Figure 4. Albuquerque ILI and east Pollen time series contrasted to winds (a,b) and average residence time of atmospheric particles as a function of particle size (c). Data for average residence time are from Anastasio and Martin (2001).

It is also notable that although not necessarily a significant factor for the tropics, at many temperate or near-temperate sites, seasonal high winds are directly in phase with periods of high ILI rates. In Albuquerque, for example, the highest influenza rates occur in the winter, which is also associated with the highest geostrophic wind rates (Figure 4b). A straightforward examination of geostrophic UCAR wind data for Aukland, New Zealand also indicates the highest wind velocities to favor September which also is a month when ILI is typically peaking.

Figure 4c illustrates the associated general residence times of bioaerosols in size categories ranging from viruses through bacteria to pollens. The size range of antibodies are also shown for added context. The figure shows that with average dimensions of approximately 0.1 microns, viruses express the longest atmospheric residency of all the categories shown. Given that atmospheric velocities are typically attributed to range from a few meters per second slightly above the planet's surface to 70 meters per second in the stratosphere, viruses lofted high in the atmosphere along certain tracks can be expected to circumnavigate the Earth up to several times a month. In contrast, pollen dimensions are several orders of magnitude larger, ranging roughly from 10 to 100 microns, and accordingly have much lower general atmospheric residence times. These particles are well known to rapidly settle out of the atmosphere simply by gravity and rainfall. Residing closer to the surface, they are also naturally expected to express greater alignment with surface winds than with geostrophic winds. Information represented in Figures 4a and 4c supports both claims. As indicated earlier, Figure 4a displays a strong correspondence for most years between surface winds and pollen loads. Figure 4b shows an equally strong correspondence between ILI percentages (red curve) and geostrophic winds (dotted green curve). Temperatures (magenta line) alone don't explain the transport circulations of either virus or pollen variates but they also show an inverse correspondence to ILI in this region as expected.

This consideration of a viral load fluctuation through changing winds also remains consistent with a pollen causal model, so long as relative residence times and scales are considered. In that scenario, a seasonal load of fresh virus material (perhaps including novel strains) associated with natural annual circulation patterns, may provide a baseline for subsequent SRV activity, and a subsequent pollen spike can then be attributed to cut that back.

4. DISCUSSION

Much like any SRV vaccine, pollen stimulates an antigenic reaction that is accompanied by the production of antibodies (e.g., Woodfolk et al., 2015; Hosoki et al., 2015). The well-known IgE antibody emergence over pollen season appears to affect all who are exposed whether or not they develop allergies (Broksted et al., 2006). These antigenic reactions from pollen are not widely credited for diminishing ILI, yet "cross reactivity" of antibodies is a common research area, and some publications have identified this attribution for IgE to counter SRVs (Smith-Norowitz et al., 2011; also indirectly, Lee et al., 2015). Historically it is also evident that ILI counts uniformly recede when pollens become airborne. The recession continues in alignment with the half-life of IgE, which is attributed to be a few months (Lawrence et al., 2016).

These connections may be spurious, but they merit consideration if only because first, no consistently accurate seasonal arguments accompany or inform current SEIR models, and second, no other climatological variable considered in Figure 3 shares this feature with vaccines. If pollen circulation provides a check upon SRVs then it may at least be conceptualized as a type of immunogen. From that perspective, hypothetical pollen immunogenic effectiveness can be compared to standard SRV vaccine products.

The comparison might favor pollen in this hypothetical context, because SRV vaccines are limited in effectiveness and scope. Broad-spectrum vaccines have been suggested as possible (Whittle et al., 2011). However, those have not reached the mainstream vaccine production process. Ultimately metrics for the effectiveness of current vaccination programs (Fukushima and Hirota, 2017, Spruijt et al, 2016) are mixed. And although vaccinations have mildly trended upwards, it remains notable that in many locations ILIs have risen dramatically over the past several years. In contrast, if pollens play a role, then a high and broad-spectrum efficacy in diminishing SRVs might then be justified based on Figure 3 alone.

Naturally many questions revolve around this notion. As previously noted, SRVs are conventionally not attributed to be impacted by pollen-induced IgE antibodies. In Figure 5a, some selected antibodies, the IgG and IgM epitopes are shown to be similar in geometry to the IgE antibody. This crude geometric comparison doesn't do justice to the extraordinary degrees of freedom and connectivity associated with the known categories of antibodies. It is simply intended to show that basic antibody components are shared universally. Numerous publications including Wharton et al. (1995) and Padavattan et al. (2009) provide detail and descriptions of the structures of IgE and many other antibodies. Figure 5 of the Padavattan et al. paper also highlights the cross reactivity between various antibody types. It shows for example that antibodies such as IgG, which are typically associated with fighting SEVs, can also bind with pollen antigens.

This limited survey of publications adds support to the geospatial correlations for a pollen immunogenic concept. However, the spectrum and nature of future work could be significant in order to confirm this concept, or to simply understand more based upon it. For example, Figure 5a addressed one of many uncertainties facing this interdisciplinary study. Another question of interest concerns the applicability of seasonality and pollens to Covid-19 like illnesses (CLIs). According to a number of recent papers, the parallel seasonality of CLIs to ILIs appears to now be firmly established (Henson et al., 2020, Moriyama et al., 2020, and Kissler, 2020). Figure 5b augments that conclusion through an examination of the CDC's CovidView dashboard and combining their CLI curve with the ILI curve for the same period of time. Notably the two variables fluctuate largely in tandem and this is also evidenced by the high correlation of 0.79 indicated within the figure panel.

Finally Figure 5c illustrates the variety of dense data sets for numerous varieties of pollen monitored at a single Albuquerque station which supported this study. We limited our investigation primarily to total counts regardless of the variety. Notably, pollens come in a diversity of shapes and sizes, ranging from spiked to smooth to incised. It would be helpful to understand much more about surface properties of pollens and the varieties and conditions that are associated with antigenic impacts and ultimately if merited, SRV reactions.

In summary, a new hypothesis that relates SRVs to geostrophic circulation coupled with pollen cycles is proposed to address the current gaps in our understanding of ILI patterns. Given the added but unexamined potential that pollens might act as a type of broad-spectrum immunogen, this research points in general to possible improvements in both ILI forecasting and ILI mitigations.

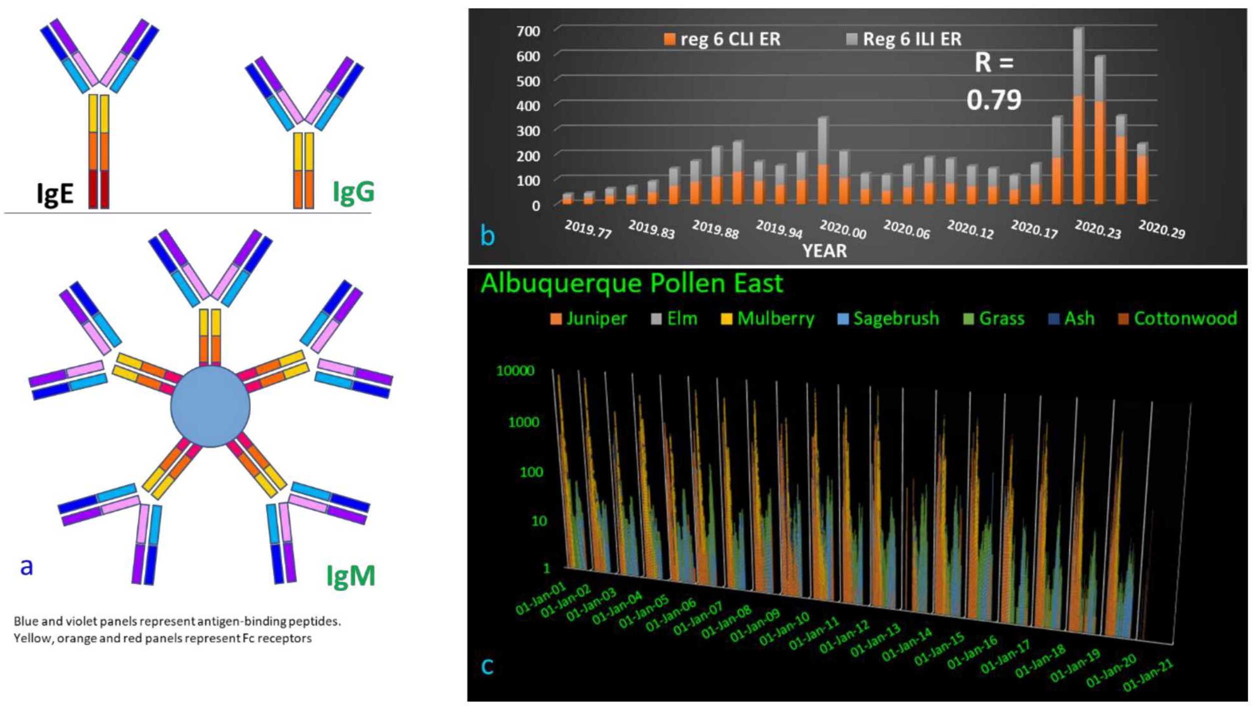

Figure 5. Uncertainty topics. a. Antibody schematics b. Comparison of recent CDC data for ILI and CLI indexes. c. Selected pollen species used in developing total pollen counts for east Albuquerque.

REFERENCES

Almeida, A., Codeço, C. and Luz, P. 2018. Seasonal dynamics of influenza in Brazil: the latitude effect. BMC Infectious Diseases. (2018) 18:695 https://doi.org/10.1186/s12879-018-3484-z

Alonso, W.J., Viboud, C., Simonsen, L., Hirano, E.W., Saufenbach, L.Z. and Miller, M.A. 2007. Seasonality of influenza in Brazil: A traveling wave from the Amazon to the Subtropics. American Journal of Epidemiology. Vol. 165, No. 12. DOI: 10.1093/aje/kwm012

Anastasio, C., and Martin, S.T., 2001. Atmospheric Nanoparticles. In NANOPARTICLES AND THE ENVIRONMENT. Banfield, J.F. and Navrotsky, A., Editors. Reviews in Minerology and Geochemistry Volume 44. Minerological Society of America, Geochemical Society. ISBN 0-939950-56-1

Behling, H. and Negrelle, R.R.B., 2006. Vegetation and pollen rain relationship from the tropical Atlantic Rain Forest in Southern Brazil. Brazilian Archives of Biology and Technology An International Journal. Vol. 49. N.4:pp. 631-642

Cannell, J J et al. "Epidemic influenza and vitamin D." *Epidemiology and infection* vol. 134,6 (2006): 1129-40. doi:10.1017/S0950268806007175

Caraballo, L., Zakzuk, J., Lee, B.W., Acevedo, N., Soh, J.Y., Sánchez-Borges, M., Hossny, E., Garcia, E., Rosario, N., Asotegui, I., Puerta, L., Sánchez, J., and Cardona, V. Particularities of allergy in the Tropics World Allergy Organization Journal (2016) 9:20 DOI 10.1186/s40413-016-0110-7

Center for Disease Control (CDC), 2020, a https://gis.cdc.gov/grasp/fluview/fluportaldashboard.html, b https://www.cdc.gov/coronavirus/2019-ncov/covid-data/covidview/04172020/covid-like-illness.html

Charu, V. Zeger, S., Gog, J., Børrnstad, O.N., Kissler, S., Simonsen, L., Brenfell, B.T. and Viboud, C. 2017. Human mobility and the spatial transmission of influenza in the United States. PLOS Computational Biology | DOI:10.1371/journal.pcbi.1005382 February 10, 2017

City of Albuquerque, Environmental Health Department. Air Quality Program. https://www.cabq.gov/airquality

Chen, G., et al., 2004. Observing the coupling effect between warm pool and "rain pool" in the Pacific Ocean. Remote Sensing of Environment, 91, 153–159. doi:10.1016/j.rse.2004.02.010

Chothe, S.K., Bhushan, G., Nissly, R.H., Yeh, YT., Brown, J., Turner, G., Fisher, J., Sewall, B.J., Reeder, D.M., Terrones, M., Jayarao, B.M., and Kuchipudi, S.V. 2017. Avian and human influenza virus compatible sialic acid receptors in little brown bats. Scientific Reports. | 7: 660 | DOI:10.1038/s41598-017-00793-6

Fukushima, W. and Hirota, Y. 2017. Basic principles of test-negative design in evaluating influenza vaccine effectiveness. Vaccine 35 (2017) 4796-4800

Greco, J.B., and Lima, A.O., 1943. The Pollen Content of the Air in Rio De Janeiro, Brazil. The Journal of Allergy and Clinical Immunology https://www.jacionline.org/article/S0021-8707(44)90160-7/pdf

Hammond, W.Q., Raddatz, R.L., and Gelskey, D.E. 1989. Impact of atmospheric dispersion and transport of viral aerosols on the epidemiology of influenza. Reviews of Infectious Diseases . Vol. 11, Number 3 May-June 1989

Henson, B. March 10, 2020. Coronavirus and Seasonality: What We Know and Don't Know https://www.wunderground.com/cat6/coronavirus-and-seasonality-what-we-know-and-dont-know

Hosoki, K., Boldogh, I., and Sur, S. 2015. Innate responses to pollen allergens. Current Opinions in Allergy Clinical Immunology. 2015 February : 15 (1): 79-88. doi:10.1097/ACI.0000000000000136.

Kissler, S.M., Tedijanto, C., Goldstein, E., Grad, Y.H. and Lipsitch, M. 2020. Projecting the transmission dynamics of SARS-CoV-2 through the postpandemic period. Science 368, 860-868

Lawrence, M.G., Woodfolk, J.a., Schuyler, A.J., Stillman, L.C., Chapman, M.D., and Platts-Mills, T.A.E., 2016. Half-life of IgE in serum and skin: Consequences for anti-IgE therapy in patients with allergic disease. Journal of Allergy and Clinical Immunology. Volume 139, Issue 2, February 2017, Pages 422-428.e4

Lee, I.K., Hwang, B.S., Kim, D.W., Kim, J.Y, Woo, E.E., Lee, Y.J., Choi, H.J., and Yun, B.S. 2016. Characterization of Neuraminidase Inhibitors in Korean *Papaver rhoeas* Bee Pollen Contributing to Anti-Influenza Activities *In Vitro*. Planta Med 2016; 82:524-529.

Legendre, M., Bartoli, J., Shmakova, L., Jeudy, S., Labadie, K., Adrait, A., Lescot, M., Poirot, O., Bertaux, L., Bruley, C., Couté, Y., Rivkina, E., Abergel, C. and Claverie, JM. 2014. Thirty-thousand-year-old distant relative of giant ocosahedral DNA viruses with a pandoravirus morphology. Proceedings of the National Academy of Sciences. Doi 10.1073/pnas.1320670111

Lofgren, E., Fefferman, N.H., Naumov, Y.N., Gorski, J. and Naumova, E.N. 2007. Influenza Seasonality: Underlying Causes and Modeling Theories Journal of Virology, June 2007, p. 5429-5436 doi:10.1128/JVI.01680-06

Moriyama, M., Hugentobler, W.J., Iwasaki, A., 2020. Seasonality of Respiratory Viral Infections. Annual Review of Virology. 2020. 7:2.1-2.19

New Mexico Department of Health. Epidemiology and Response Division. www.nmhealth.org

Padavattan, S., Flicker, S., Schirmer, T., Madritsch, C., Randow, S., Reese, G., Vieths, S., Lupinek, C., Ebner, C., Valenta, R. and Markovic-Housley, Z. 2009. High-affinity IgE recognition of a conformational Epitope of the major respiratory allergern Phl p 2 as revealed by X-Ray crystallography. The Journal of Immunology 2009: 182:2141-2151. doi: 10.4049/jimmunol.0803018

Reche, I., D'Orta, G., Mladenov, N., Winget, D.M., and Suttle, C.A. 2018. Deposition rates of viruses and bacteria above the atmospheric boundary layer. The ISME Journal Springer Nature https://doi.org/10.1038/s41396-017-0042-4

Shaman J, Pitzer V, Viboud C, Lipsitch M, Grenfell B. Absolute Humidity and the Seasonal Onset of Influenza in the Continental US. *PLoS Curr*. 2009;2:RRN1138. Published 2009 Dec 18. doi:10.1371/currents.RRN1138

Shaman J, Kandula S, Yang W, Karspeck A (2017) The use of ambient humidity conditions to improve influenza forecast. PLoS Comput Biol 13(11): e1005844.https://doi.org/10.1371/journal.pcbi.1005844

Smith, D.J., 2013. Microbes in the upper atmosphere and unique opportunities for astrobiology research. Astrobiology. Volume 13, Number 10

Smith-Norowitz, T.A., Kusonruksa, M., Wong, D., Norowitz, M.M., Joks, R., Durkin, H.G., and Bluth, M.H., 2012. Long-term persistence of IgE anti-influenza A HIN1 virus antibodies in serum of children and adults following influenza A vaccination with subsequent H1N1 infection: a case study. J. Inflamm Res 20102, 5:111-6 doi: 10.2147/JIR. S34152.

Spruijt, I.T., de Lange, M.M.A., Dijkstra, F., Donker, G.A., and van der Hoek, W. 2016. Long-Term Correlation between Influenza Vaccination Coverage and Incidence of Influenza-Like Illness in 14 European Countries. PLOS ONE | DOI:10:10.1371/journal.pone.01 63508 September 29, 2016

Su W, Liu T, Geng X, Yang G. 2020. Seasonal pattern of influenza and the association with meteorological factors based on wavelet analysis in Jinan City, Eastern China, 2013–2016. PeerJ 8:e8626 https://doi.org/10.7717/peerj.8626

Tamerius, J., Nelson, M.I., Zhou, S.Z., Viboud, C., Miller, M.A., and Alonso, W.J. 2011. Global Influenza Seasonality: Reconciling Patterns across Temperate and Tropical Regions. Environmental Health Perspectives Volume 119 Number 4 Review April 2011

Tamerius, J.D., Shaman, J., Alonso, W.J., Bloom-Feshbach, K., Uejio, C.K, Comrie, A., and Viboud, C. 2013. Environmental Predictors of Seasonal Influenza Epidemics across Temperate and Tropical Climates. PLoS Pathog 9(3): e1003194. doi:10.1371/journal.ppat.1003194

University of California at Riverside (UCAR) 2015 integration of ERAI satellite reanalyses products http://www.cgd.ucar.edu/cas/catalog/newbudgets/index.html#ERBEFs – file 'ERAI.LEDIV.1979–2014.nc

Wallace, M.G., 2019, Application of lagged correlations between solar cycles and hydrosphere components towards sub-decadal forecasts of streamflows in the Western US. Hydrological Sciences Journal, Oxford UK Volume 64 Issue 2. doi: 10.1080/02626667.2019.

Whittle, J.R.R., Zhang, R., Khurana, S., King, L.R., Manischewitz, J., Golding, H., Dormitzer, P.R., Haynes, B.F., Walter, E.B., Moody, M.A., Kepler, T.B., Liao, HX, and Harrison, S.C. 2011. Broadly neutralizing human antibody that recognizes the receptor-binding pocket of influenza virus hemagglutinin Proceedings of the National Academy of Sciences Aug 2011, 108 (34) 14216-14221; DOI: 10.1073/pnas.1111497108

Whon, T.W., Kim, MS., Roh, S.W., Shin, NR., Lee, HW., and Bae, JW. 2012. Metagenomic Characterization of Airborne Viral DNA Diversity in the Near-Surface Atmosphere. Journal of Virology p. 8221-8231

Woodfolk, J.A., Commins, S.P., Schuyler, A.J., Erwin, E.A. and Platts-Mills, T.A.E. 2015. Allergens, sources, particles, and molecules: Why do we make IgE responses? Allergology International 64 (2015) 295-303

World Health Organization (WHO) 2020. https://www.who.int/influenza/ gisrs_laboratory/ flunet/en/

Zhang, Y. Bielory, L., Cai, T., Mi Z. and Georgopoulus, P. 2015. Predicting onset and duration of airborne allergenic pollen season in the United States. Atmospheric Environment 103 (2015) 297-306.

Appendix

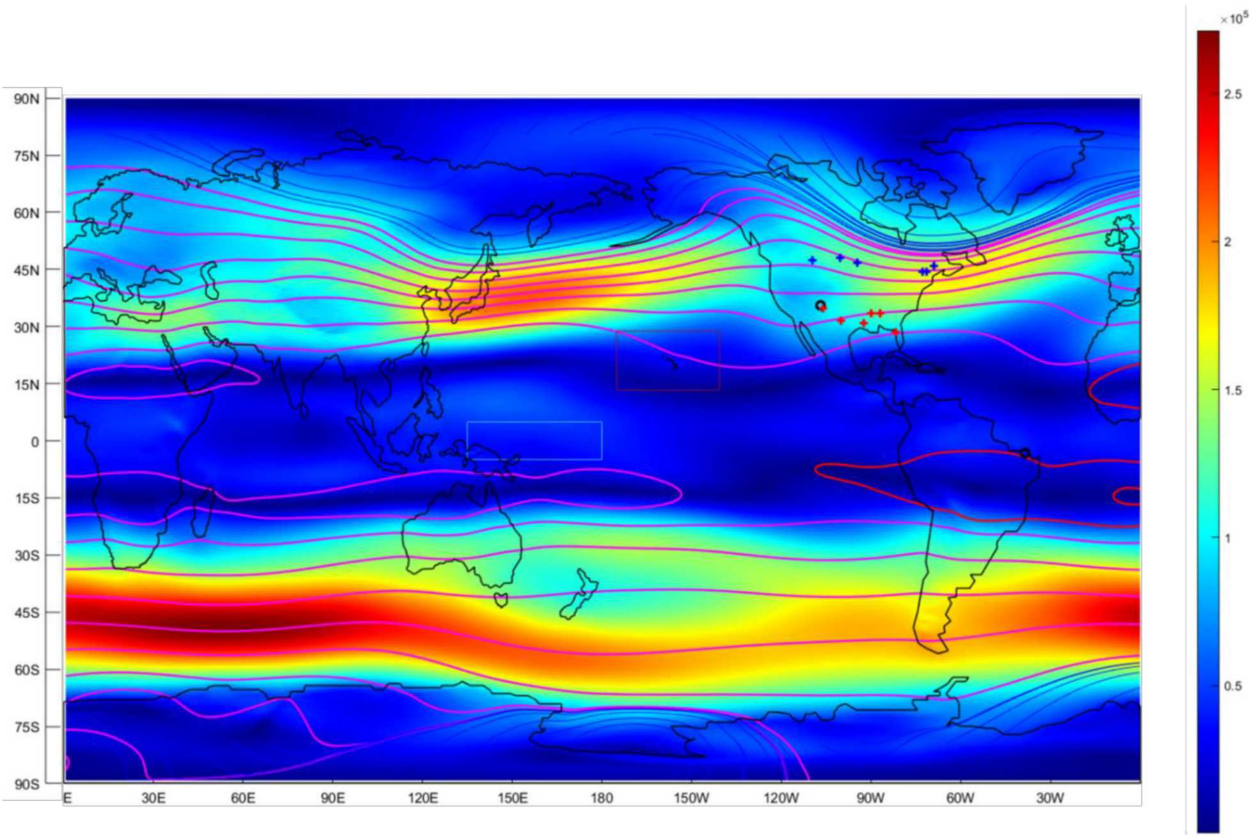

Figure A1 Global Geostrophic Winds Units: kg m^{-1} s^{-1}, average of 36 years of UCAR-integrated ERAI monthly records Streamlines: magenta lines emerge from west boundary. Red lines emerge from east boundary. Blue lines originate from approximately Arctic and Antarctic Circles.

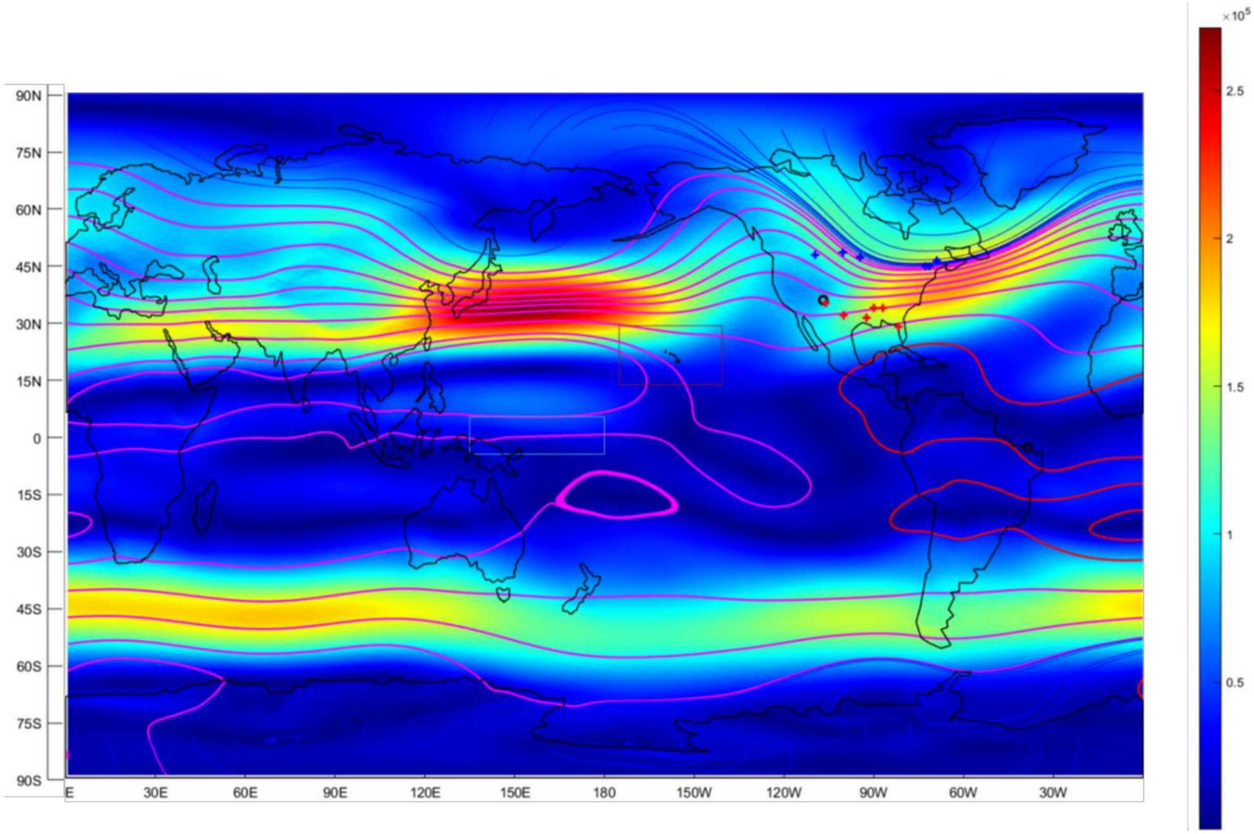

Figure A2. **Global Geostrophic Winds kg m^{-1} s^{-1} , January Avg from UCAR-ERAI 1979 through 2014 Streamlines: magenta lines emerge from west boundary. Red lines emerge from east boundary. Blue lines originate from approximately Arctic and Antarctic Circles.**

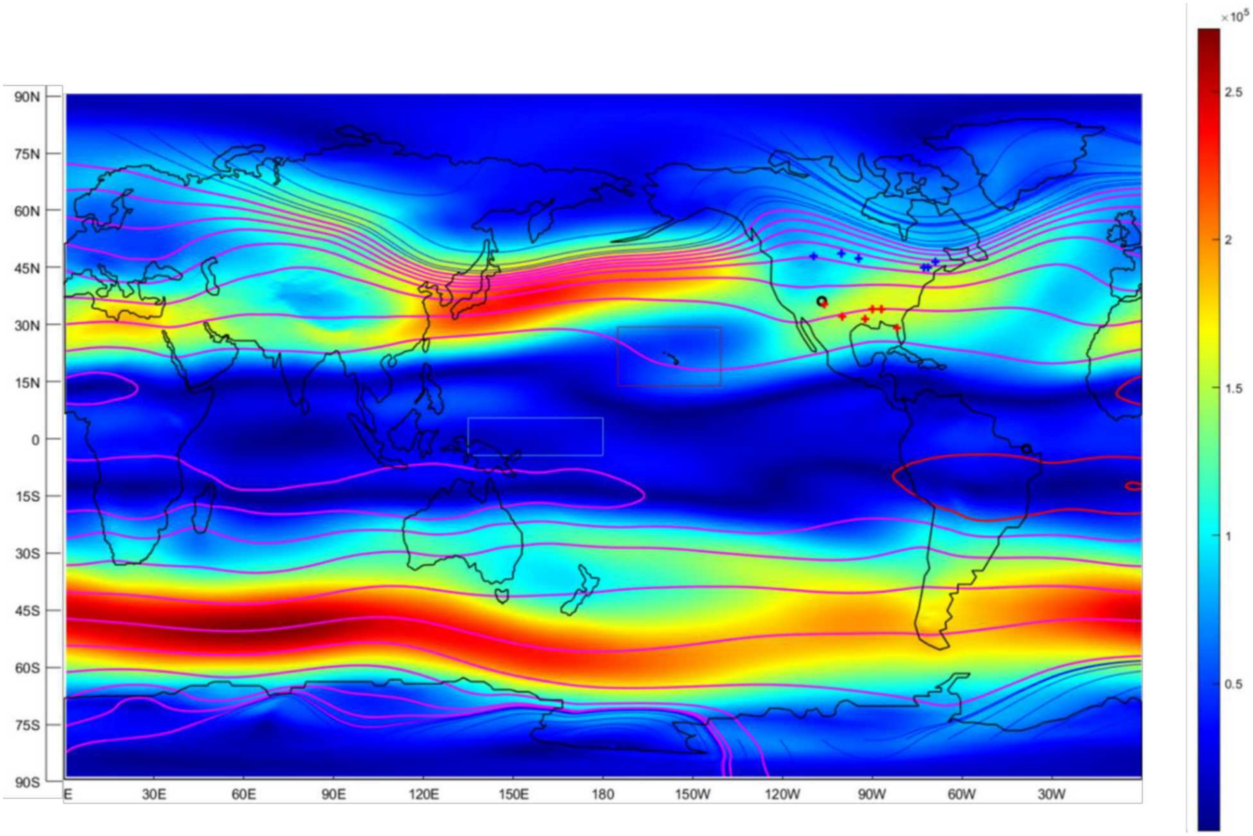

Figure A3. Global Geostrophic Winds kg m^{-1} s^{-1} , April Avg from UCAR-ERAI 1979 through 2014 Streamlines: magenta lines emerge from west boundary. Red lines emerge from east boundary. Blue lines originate from approximately Arctic and Antarctic Circles.

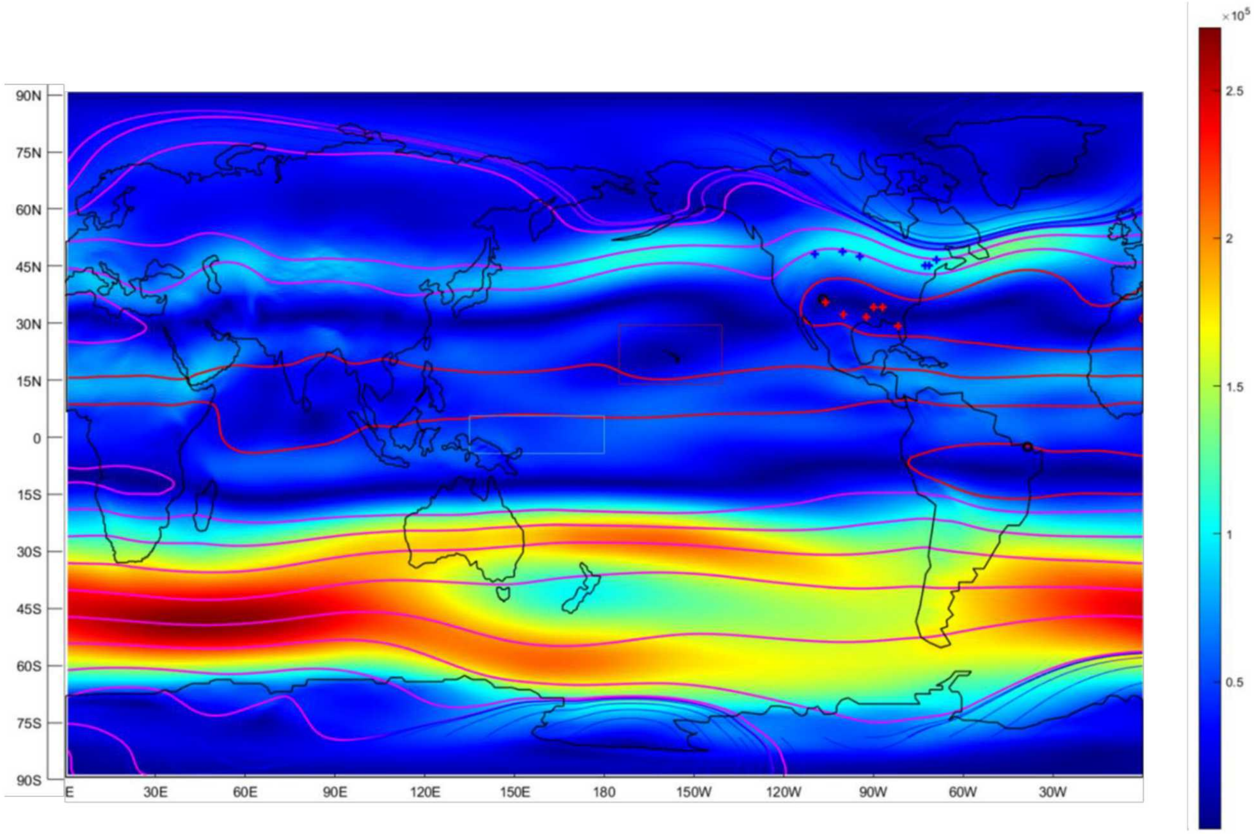

Figure A4. Global Geostrophic Winds kg m^{-1} s^{-1} , July Avg from UCAR-ERAI 1979 through 2014 Streamlines: magenta lines emerge from west boundary. Red lines emerge from east boundary. Blue lines originate from approximately Arctic and Antarctic Circles.

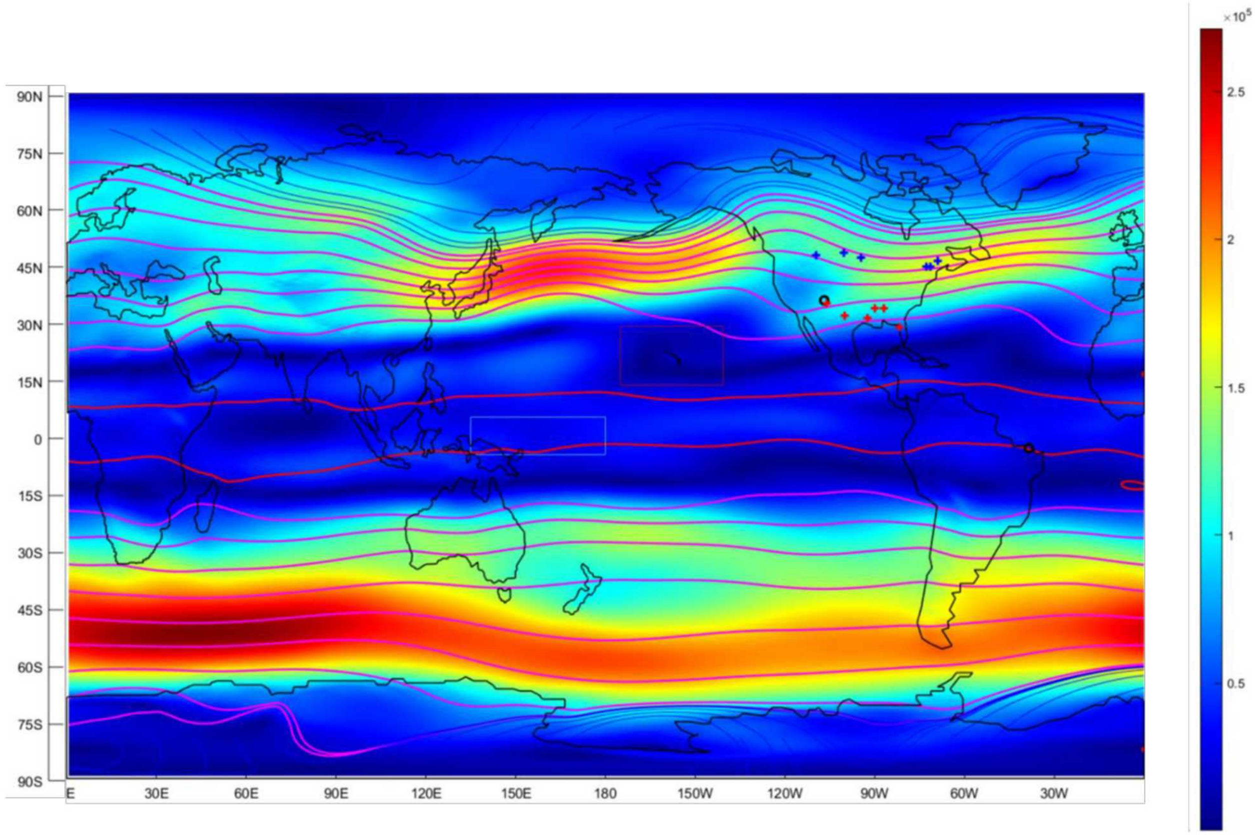

Figure A5. **Global Geostrophic Winds kg m^{-1} s^{-1} , October Avg from UCAR-ERAI 1979 through 2014 Streamlines: magenta lines emerge from west boundary. Red lines emerge from east boundary. Blue lines originate from approximately Arctic and Antarctic Circles.**

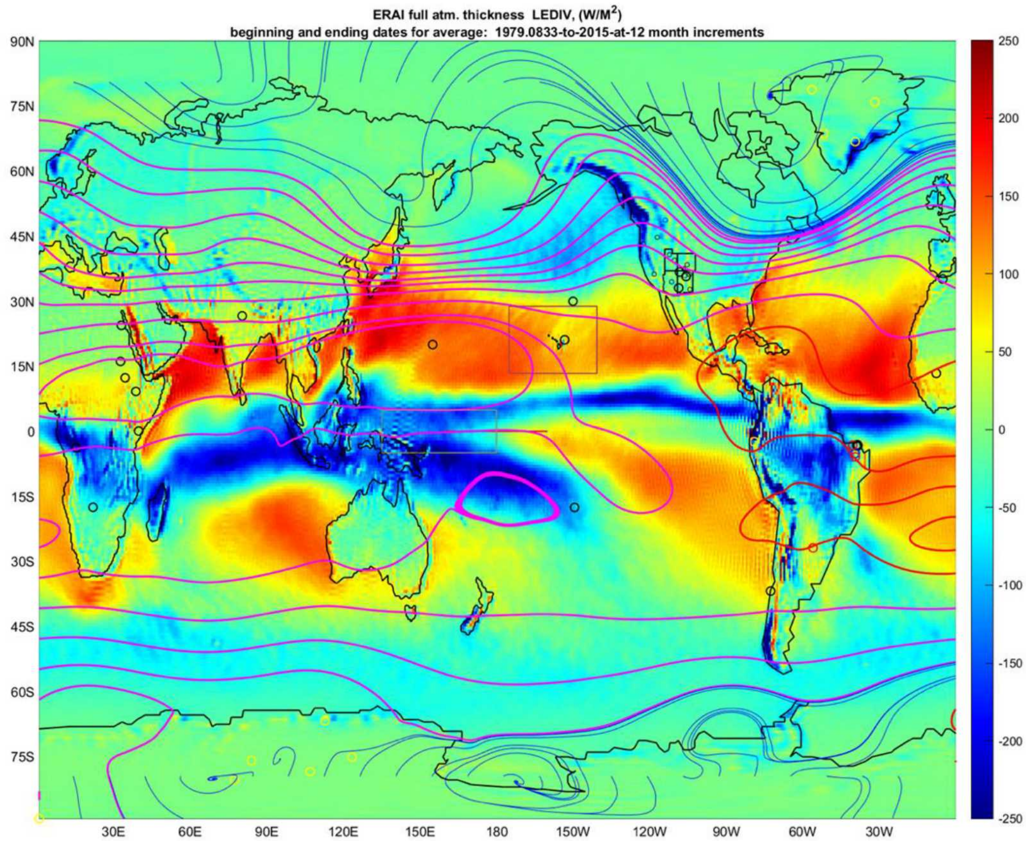

Figure A6. Global Geostrophic LDEV, January Avg from UCAR-ERAI 1979 through 2014 (W/m^2). Streamlines: magenta lines emerge from west boundary. Red lines emerge from east boundary. Blue lines originate from approximately Arctic and Antarctic Circles.

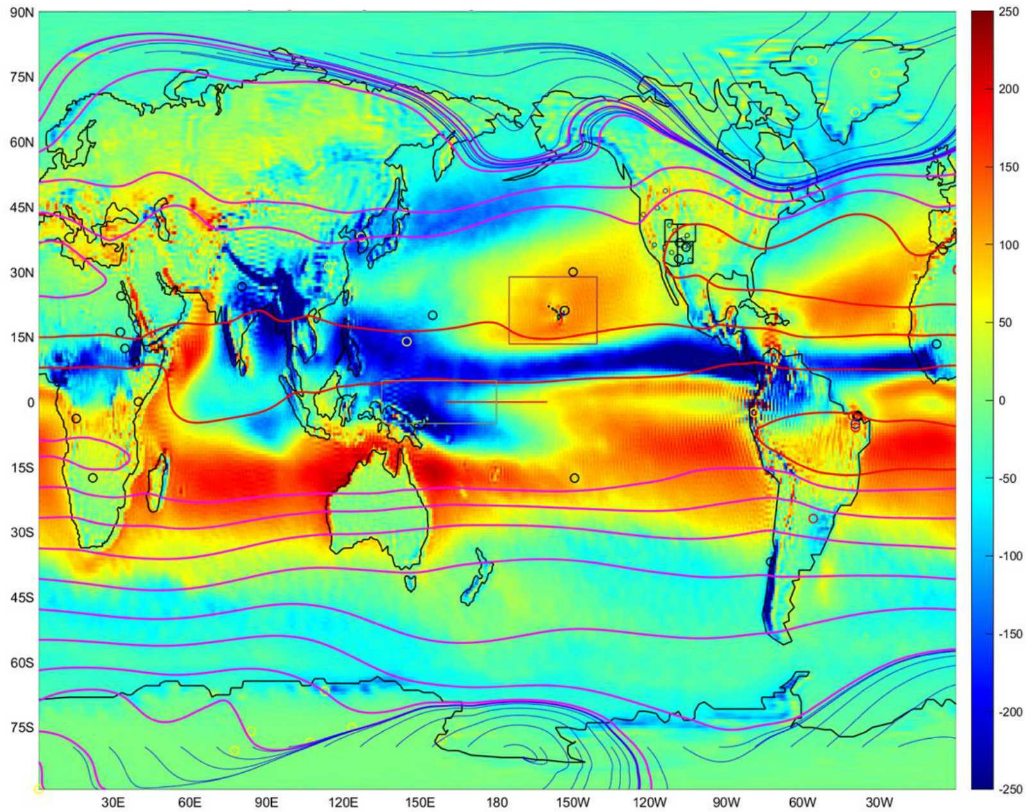

Figure A7. Global Geostrophic LDEV, July Avg from UCAR-ERAI 1979 through 2014 (W/m^2) Streamlines: magenta lines emerge from west boundary. Red lines emerge from east boundary. Blue lines originate from approximately Arctic and Antarctic Circles.

DISTRIBUTION

Email—Internal

Name	Org.	Sandia Email Address
Technical Library	01977	sanddocs@sandia.gov

Email—External (encrypt for OUO)

Name	Company Email Address	Company Name

Hardcopy—Internal

Number of Copies	Name	Org.	Mailstop

Hardcopy—External

Number of Copies	Name	Company Name and Company Mailing Address

This page left blank

This page left blank

Sandia National Laboratories

Sandia National Laboratories is a multimission laboratory managed and operated by National Technology & Engineering Solutions of Sandia LLC, a wholly owned subsidiary of Honeywell International Inc. for the U.S. Department of Energy's National Nuclear Security Administration under contract DE-NA0003525.